Numerical Simulation of Behaviors of Settling Fish Aggregation Device

by

Yoshiharu MATSUMI and Akira SEYAMA

Department of Ocean Civil Engineering

(Received September 1, 1986)

This study aims at clarifying the effective method to set up the fish aggregation device(FAD) thrown down from a ship on the designed position most accurately, the numerical simulation techniques are developed to analyze the behaviors of the settling FAD in consideration of the effect of vortices generated behind it.

Key words : Fish aggregation device, Settling behaviors, Implusive force at landing, Discrete vortex approximation, Source distribution method,

1. INTRODUCTION

A fish aggregation device (FAD) is a structure to gather fishes, usually placed on the sea bottom of a depth from about 30 to 100 meters. Although the properties of FAD which gather fishes have not been sufficiently clarified yet, phenomena such as vortex formation and its shedding induced by FAD have been pointed out to be the important hydraulic factors for aggregating fishes. In the case of a multi-FAD system, the efficiency of the individual FAD to gather fishes is amplified if the FAD system have an effect of multiplication. This paper investigates if the FAD system has above effect, and the optimal lay out of the FAD which activate the system most.

The FAD system is mainly constructed by throwing them down from a ship to lay out on the fishing ground. It is difficult to set up the FAD in the right position, since a settling motion of FAD in the fluid is consisted by following three complex motions (i.e. an oscillatory motion in horizontal direction, a rotational motion and vertical drop). Because of the position errors induced in the set up, the work of the system on gathering fishes may not be demonstrated sufficiently. Hence, it becomes very important to make clear the settling behaviors of FAD so as to carry out their accurate settlings on the designed position.

On the other hand, from the strength point of view, the crushing behavior of FAD is closely concerned with velocity, angular velocity and posture at landing. Nakamura, et al.[1] and Kono[2] discussed the impulsive force exerted on the FAD induced by the settling motion in the vertical direction. However, the angular velocity and the posture of FAD which seem to dominate fully in the total impulsive force exerted on the FAD at landing have not been considered in these studies.

In this study, in other to clarify (1) the effective method to set up FADs on designed positions most accurately , (2) the relation between the allowable scatter range of the landing FAD on the sea bottom and the initial condition of its posture at the throwing, the numerical simulation technique which can analyze behaviors of the setting FAD is developed in connection with the effect of vortices generated behind the FAD. The FAD treated in this study is a cubic type with a hollow inside and gaps on the surface. This type of FAD has been used most frequently.

2. MATHEMATICAL DESCRIPTION OF THE SIMULATION METHOD

The oscillatory motion of a settling FAD in a periodic wave is affected

by the instantaneous fluctuations of the pressure distribution around it, because of the vortices generated from it and the wave motion. Hence, in this numerical simulation of the settling FAD, the fluid resistance exerted on it is estimated firstly by integrating the pressure distribution around the surface of the FAD. This surrounding pressure distribution is calculated from the simulated flow pattern around the settling FAD. Secondly, the oscillatory motion of the settling FAD at every moment is numerically calculated from the equation of motion.

2-1 Description of the fluid field around the settling FAD

The discrete vortex approximation which has been suggested by a number of works as a powerful method for the analysis of the flow pattern around a bluff-based body with separated flow, is used to simulate the flow pattern around the settling FAD in the present study. The singularity method[3] (the source distribution method) is adopted to formulate the boundary condition on the surface of the FAD.

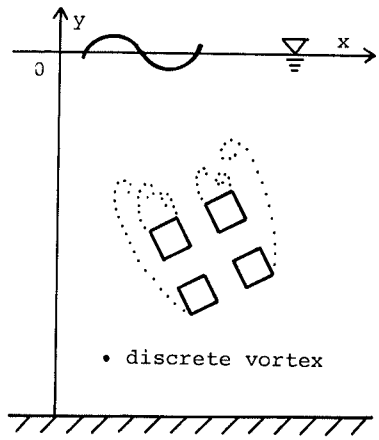

Fig.1 Schematic figure of flow field around settling FAD.

In the case of two-dimensional wave field as shown in Fig.1, the free surface in the wave field is replaced by the fixed rigid surface, since it can be assumed that the wave induced by the vortex generation from the settling FAD is the long periodic wave. The condition ($\partial\phi/\partial y=0$) is satisfied at any position on the free surface, in which ϕ is the velocity potential for the flow around the FAD. Then, the appropriate complex potential for the discrete vortex and for the strength of the source point can be determined using the Schwartz-Christoffel transformation to project an upper half of the λ-plane with the boundary along the real axis into the interior region between the

boundaries in the z-plane (see Fig.2). The λ-plane is transformed into the physical z-plane by the function

$$\frac{dz}{d\lambda} = \kappa \frac{1}{\lambda} \tag{1}$$

or

$$z = x+iy = \kappa \log\lambda + c \tag{2}$$

where K is the constant determined by the water depth, and C is a integral constant. Since $\lambda=-1$ at $z=0$ and $\lambda=1$ at $z=-ih$ in which $i=\sqrt{-1}$ and h is the water depth, Eq.(2) is rearranged in term of z as,

$$\lambda = -\exp(c_0 z) \qquad (c_0=\pi/h) \tag{3}$$

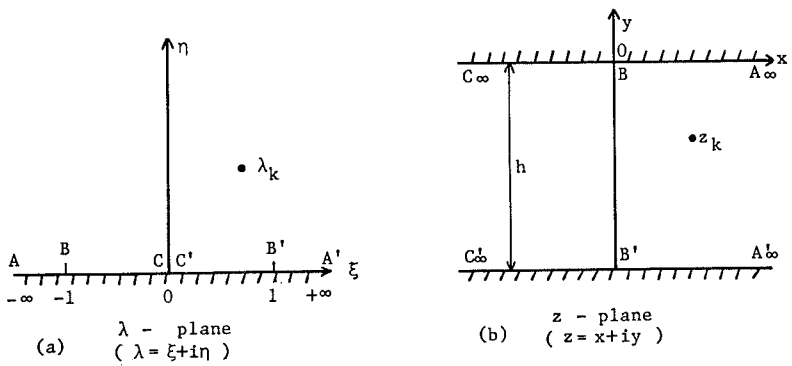

Fig.2 (a) transformed plane λ ; (b) physical plane z.

The complex potential ($\omega_{v\lambda k}$) of the discrete vortex (λ_k) in λ-plane (Fig.2) is given by the following equation in terms of the imaginary discrete vortex which is necessary to maintain the boundary condition of zero flow across the real axis in λ-plane.

$$\omega_{v\lambda_k} = \frac{i\Gamma_k}{2\pi}\{\log(\lambda-\lambda_k) - \log(\lambda-\bar{\lambda}_k)\} \tag{4}$$

where Γ_k and λ_k are the circulation and the complex coordinate of the vortex respectively, the circulation is defined as positive being clockwise, and the over bar denotes the complex conjugate. Substituting Eq.(3) into Eq.(4), the complex potential (ω_{vzk}) in z-plane is introduced as

$$\omega_{vz_k} = \frac{i\Gamma_k}{2\pi}\{\log(e^{c_0 z_k}-e^{c_0 z}) - \log(e^{c_0 \bar{z}_k}-e^{c_0 z})\} \tag{5}$$

where z_k is the complex coordinate of the vortex in z-plane. With the same way

that used for the discrete vortex (eq.(4)), the complex potential (ω_{Rz_m}) of the source point in z-plane is given by

$$\omega_{RZ_m} = \frac{D(z_m)}{2\pi}\{\log(e^{C_0 z_m}-e^{C_0 z})+\log(e^{C_0 \bar{z}_m}-e^{C_0 z})\} \tag{6}$$

where z_m and $D(z_m)$ are a location and a strength of the source point respectively.

When the flow around the settling FAD in z-plane consists of a periodic wave, Q vortices with some circulations generated from P separation points, and the flow from the source points on the FAD surface, the complex potential ω_z at the points z in z-plane is given by

$$\begin{aligned}\omega_Z &= \phi_Z+i\psi_Z = \omega_W+\omega_{VZ}+\omega_{RZ}\\ &= \omega_W+\frac{i}{2\pi}\sum_{j=1}^{Q}\sum_{k=1}^{P}\Gamma_{jk}\{\log(e^{C_0 z_{jk}}-e^{C_0 z})-\log(e^{C_0 \bar{z}_{jk}}-e^{C_0 z})\}\\ &\quad+\frac{1}{2\pi}\oint_C D(z_m)\{\log(e^{C_0 z_m}-e^{C_0 z})+\log(e^{C_0 \bar{z}_m}-e^{C_0 z})\}dc\end{aligned} \tag{7}$$

where ϕ_z and ψ_z are the velocity potential and the stream function for the total flow in the z-plane respectively, ω_w is the complex velocity potential of the wave, $\oint_C$ represents the contour integral along the surface C of the settling FAD, and z_m is the point on C.

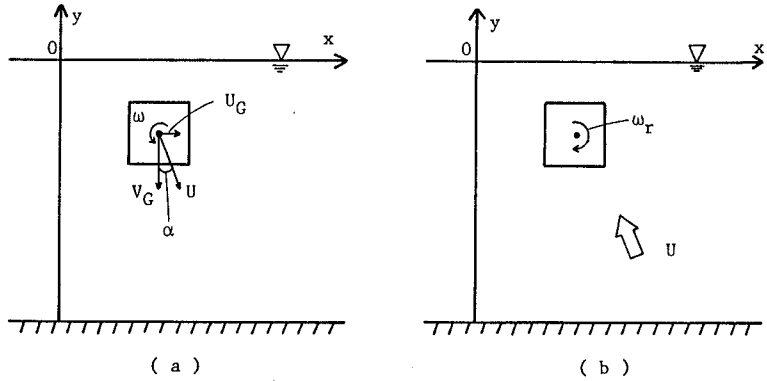

Fig.3 (a) flow around settling FAD ;
(b) flow around fixed FAD.

The strength $D(z_m)$ of the source point is determined by the boundary condition (i.e. the fluid velocity normal to FAD surface is zero). When the FAD is settling with speed $U(=\sqrt{U_G^2+V_G^2})$ at the angle α $(=\tan^{-1}U_G/V_g)$ and with an angular velocity ω as shown in Fig.3(a), taking the origin at the center of the settling FAD, the FAD motion can be fixed in such a flow field that is

consisted of the uniform flow with the mentioned velocity at an angle α with respect to y axis and the rotational flow generated by the FAD rotation. Therefore, the identical equation of the strength $D(z_m)$ of the source point becomes as

$$\mathrm{Real}\left[\frac{\partial \omega_{RZ}}{\partial n}\right] = -(U_c n_x + V_c n_y) \tag{8}$$

where n is a unit vector outward normal to the surface of the FAD, n_x and n_y are the x and y components of the vector respectively, u_c and v_c are the x , y components of the velocity in the n direction. Using the normal differential $(\partial/\partial n = \partial/\partial x \cdot n_x + \partial/\partial y \cdot n_y)$ and Eq.(6), the left-hand side term in Eq.(8) becomes as

$$\mathrm{Real}\left[\frac{\partial \omega_{RZ}}{\partial n}\right] = \oint_C D(Z_m)\frac{C_0}{4\pi}\left[\left\{2+\frac{SH(x,x_m)}{I(x,y;x_m,y_m)}+\frac{SH(x,x_m)}{I(x,y;x_m,-y_m)}\right\}n_x + \left\{\frac{SN(y,y_m)}{I(x,y;x_m,y_m)}+\frac{SN(y,-y_m)}{I(x,y;x_m,-y_m)}\right\}n_y\right]dc \tag{9}$$

where SN, SH and I are the following function.

$$SN(a,b)=\sin\{C_0(a-b)\}$$

$$SH(a,b)=\sinh\{C_0(a-b)\}$$

$$I(a,b;c,d)=\cosh\{C_0(a-c)\}-\cos\{C_0(b-d)\}$$

Putting

$$\begin{aligned} U_C &= (U_W+U_V+U_U+U_r)\big|_{Z=Z_C} \\ V_C &= (V_W+V_V+V_U+V_r)\big|_{Z=Z_C} \end{aligned} \tag{10}$$

The velocity components are given as follows, respectively.

$$\begin{aligned} U_V &= \frac{C_0}{4\pi}\sum_{j=1}^{Q}\sum_{k=1}^{P}\Gamma_{jk}\left\{\frac{SN(y,y_{jk})}{I(x,y,x_{jk},y_{jk})}-\frac{SN(y,-y_{jk})}{I(x,y;x_{jk},-y_{jk})}\right\} \\ V_V &= \frac{C_0}{4\pi}\sum_{j=1}^{N}\sum_{k=1}^{P}\Gamma_{jk}\left\{\frac{SH(x,x_{jk})}{I(x,y;x_{jk},y_{jk})}-\frac{SH(x,x_{jk})}{I(x,y;x_{jk},-y_{jk})}\right\} \\ U_U &= U\sin\alpha\ , \quad V_U = U\cos\alpha \\ U_r &= \omega(y-y_G)\ , \quad V_r = -\omega(x-x_G) \\ U_w &= \partial\phi/\partial x\ , \quad V_w = \partial\phi/\partial y \end{aligned} \tag{11}$$

where (u_W,v_W), (u_V,v_V), (u_U,v_U) and (u_r,v_r) are the velocity components induced by the periodic wave, the discrete vortices, the uniform flow and the rotational flow, respectively, x_G and y_G are the position of the gravitational center of the FAD in the moving coordinate system.

In the numerical calculation of Eq.(8), the surface C of the FAD is divided into N sections of length ΔC_m (m=1 ~ N) (as shown in Fig.4), and the source point is set on the center of the each section. Then the corner of the FAD is approximated with a circular arc of a radius r=0.02a, in which a is the length of the FAD side. Hence, the strength $D(z_m)$ of the individual source points are given as solutions of the following equations.

$$\sum_{m=1}^{N} D(z_m)A_{jm}=-\{u_c(z_m)n_{xj}+v_c(z_m)n_{yj}\} \qquad j=1\sim N \qquad (12)$$

where

$$A_{jm}=\frac{C_0}{4\pi}[\{\frac{SH(x_j,x_m)}{I(x_j,y_j;x_m,y_m)}+\frac{SH(x_j,y_j)}{I(x_j,y_j;x_m,-y_m)}+2\}n_{xj}$$
$$+\{\frac{SN(x_j,y_m)}{I(x_j,y_j;x_m,y_m)}+\frac{SN(y_j,-y_m)}{I(x_j,y_j;x_m,-y_m)}\}n_{yj}]\Delta C_m \qquad \text{at } j\neq m$$

$$A_{jm}=\frac{C_0}{4\pi}[2n_{xj}+\frac{\sin 2c_0y_m}{1-\cos 2c_0y_m}n_{yj}]\Delta C_m+\frac{1}{2} \qquad \text{at } j=m$$

in which n_{xj} and n_{yj} are the x , y components of the normal vector n of the j-th section.

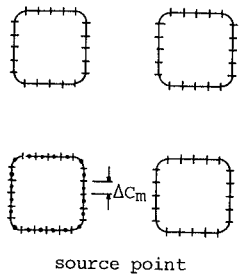

Fig.4 Segmentation of FAD model side and location of source points.

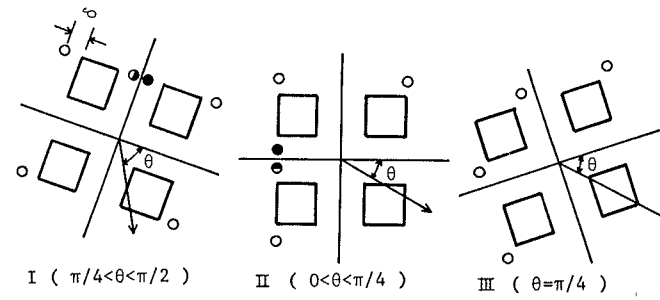

Fig.5 Initial positions of nascent vortices.

In Eq.(7), the velocities of the vortices are decided from the kinematic condition for the discrete vortices (i.e. A marked vortex is affected only from the periodic wave and the other vortices). Therefore, the velocity components u_{jk}, v_{jk} of the j-th vortex generated from the k-th separation point, are expressed as

$$u_{jk}-iv_{jk}=\frac{d}{dz}\{\omega_z-\frac{i\Gamma_{jk}}{2\pi}\log(e^{c_0z}-e^{c_0z_{jk}})\}\Big|_{z=z_{jk}} \qquad (13)$$

If there are QP pieces of discrete vortices simultaneously around the settling FAD, a set of QP ordinary differential equations are derived as equations of

the kinematic conditions for the discrete vortices.

In Eq.(13), the unknown initial position of the nascent vortex and the circulation of vortices are included. There have been no established method, however, to calculate the initial position of a nascent vortex, its position has been determined with (A) the Kutta condition at the edge of the body or (B) the boundary layer thickness. In this study, (B) is adopted, and the six nascent vortices are fixed firstly at s_1, s_2, s_3, s_4, s_5, s_6 as shown in Fig.5. These points are located at the distance of δ (boundary layer thickness which is determined by $\delta=\sqrt{\nu T/\pi}$ in which ν is the kinematic viscosity coefficient and T is the period of the wave) from the separation points of the FAD. Each position of the nascent vortex is changed with the relation between the angle of the FAD and the settling direction. The three separation patterns of the boundary layer are treated in this study as shown in Fig.5. Secondly, the circulation of the nascent vortex is calculated with the Roshko's approximate equation[4]. The damping effect of the vortex due to the turbulent diffusion and the fluid viscosity is neglected. Taking the direction of the rotation of vortices into consideration, the circulation of the nascent vortex is given by

$$\partial\Gamma/\partial t = U_s|U_s|/2 \tag{14}$$

where U_s is a fluid velocity at the initial position of the nascent vortex. Although some vortices induce large velocities when they approach each other because we neglect of the viscosity, this phenomenon is avoided by replacing the distributed discrete vortices with the Rankine vortex. The core radius of the Rankine vortex is given by $|\Gamma_{ij}|/2\pi U_s$[5] in this study.

2-2 Fluid resistance on the settling FAD

The fluid resistance exerted on the settling FAD can be obtained by integrating the pressure distributions around it, which is given in terms of $\partial\phi_z/\partial t$, u and v on the FAD surface ($z=z_c$) as

$$P_{Z=Z_c}=\{-\rho\left(\frac{\partial\phi_z}{\partial t}\right)-\frac{\rho(u^2+v^2)}{2}\}\Big|_{Z=Z_c} \tag{15}$$

where ρ is the fluid density. The first term of Eq.(15) is given by

$$\frac{\partial\phi_z}{\partial t}\Big|_{Z=Z_c} = \mathrm{Real}\left[\left(\frac{\partial\omega_W}{\partial t}+\frac{\partial\omega_{RZ}}{\partial t}+\frac{\partial\omega_{VZ}}{\partial t}\right)\Big|_{Z=Z_c}\right] \tag{16}$$

Since the position z_{jk} of the discrete vortices, its strength $D(z_m)$ and the position of the source points are functions of time in Eq.(16). This equation is written in the form

$$\frac{\partial \phi_Z}{\partial t}\Big|_{Z=Z_C} = \mathrm{Real}\Big[\Big(\frac{\partial \omega_W}{\partial t}+\frac{\partial D(Z_m)}{\partial t}\{G_{RR}(Z,Z_m)+G_{RK}(Z,\bar{Z}_m)\}$$
$$+D(Z_m)\Big\{\frac{\partial G_{RR}(Z,Z_m)}{\partial Z_m}\cdot\frac{\partial Z_m}{\partial t}+\frac{\partial G_{RK}(Z,\bar{Z}_m)}{\partial \bar{Z}_m}\cdot\frac{\partial \bar{Z}_m}{\partial t}\Big\}$$
$$+\frac{\partial \omega_{VZjk}}{\partial Z_{jk}}\cdot\frac{\partial Z_{jk}}{\partial t}+\frac{\partial \omega_{V\bar{Z}jk}}{\partial \bar{Z}_{jk}}\cdot\frac{\partial \bar{Z}_{jk}}{\partial t}\Big)\Big|_{Z=Z_C}\Big] \qquad (17)$$

where

$$G_{RR}(Z,Z_m) = \frac{1}{2\pi}\sum_{m=1}^{N}\log(e^{C_0 Z_m}-e^{C_0 Z})$$
$$G_{RK}(Z,\bar{Z}_m) = \frac{1}{2\pi}\sum_{m=1}^{N}\log(e^{C_0 \bar{Z}_m}-e^{C_0 Z})$$
$$\omega_{VZ_{jk}} = \sum_{j=1}^{Q}\sum_{k=1}^{P}\frac{i\Gamma_{jk}}{2\pi}\log(e^{C_0 Z_{jk}}-e^{C_0 Z})$$
$$\omega_{V\bar{Z}_{jk}} = -\sum_{j=1}^{Q}\sum_{k=1}^{P}\frac{i\Gamma_{jk}}{2\pi}\log(e^{C_0 \bar{Z}_{jk}}-e^{C_0 Z})$$

The second terms of Eq.(15) is given by

$$(u^2+v^2)\Big|_{Z=Z_C} = \left|(\partial\omega_Z/\partial z)\right|^2\Big|_{Z=Z_C} \qquad (18)$$

$\partial D(Zm)/\partial t$ in Eq.(17) can be calculated by differentiating Eq.(8) with respect to time t, the differentiated equation is analyzed in the same manner as the above-mentioned method for the strength of the source point.

The horizontal and the vertical fluid resistance F_x, F_y exerted on the settling FAD are given as follows lastly.

$$F_x = -\oint_C P n_x \, dC$$
$$F_y = -\oint_C P n_y \, dC \qquad (19)$$

2-3 The equations of motion of the settling FAD

Referring to Fig.6, the equations of horizontal, vertical and rotational motion for the settling FAD are given as

$$M\frac{du}{dt} = \sum_{i=1}^{4} F_{xi}$$
$$M\frac{dv}{dt} = \sum_{i=1}^{4}\{F_{yi} - (M'-M_W')g\} \qquad (20)$$
$$I_r\frac{dw}{dt} = \sum_{i=1}^{4}(x_i' F_{yi} - y_i' F_{xi})$$

where M is a mass of the FAD per unit thickness, M' and M' are masses of a piece of slender body and fluid (per unit thickness) displaced by the piece, g

is the gravity acceleration, and Ir is an inertia moment of the FAD. x_i' and y_i' are the distance from the center of the FAD cross-section to the center of an i-th piece in the x and y direction respectively.

In the numerical calculations, the second-order Runge-Kutta method was used to calculate the velocity of the discrete vortices and the motion of the settling FAD. The selection of an optimum time interval was of primary importance in achieving a relatively insensitive time step. After the preliminary calculations, the results reported herein were carried out with time-step t=0.05s.

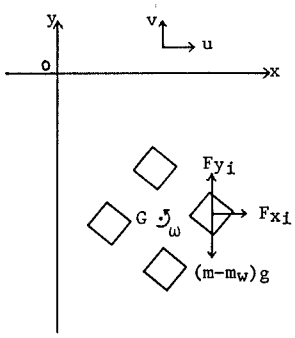

Fig.6 Fluid resistance on settling FAD.

3. DISCUSSION

At the first stage of the study, the experiments and the calculations for the settling FAD in a still water were performed, in order to obtain basic data to apply the present theory for the settling FAD in a periodic wave field.

The experiments were carried out using a water tank of the cross section of 1m x 1m and 2m in depth to observe the behaviors of the settling FAD. Two kinds of FAD with the void ratios γ=64 and 84% were used. The FAD the cross section of which is 5cm x 5cm consists of four pieces of slender rectangular (1.5cm x 1.5cm in the cross section) bodies. The photographs of the settling figures of the FAD were taken on a same film using a strobe flash, the interval time of the flash is 0.2s. From the experiments, the behaviors of the settling FAD with γ=63% may be classified into three patterns as shown in Fig.7. In Fig.7(I), form the 5-th to 7-th positions of the FAD, it settles with the clockwise rotation, and from the 8-th to the 25-th positions it settles in nearly right down direction with an inclined posture to the still water surface at angle of about 45°. In Fig.7(II) the direction of the settling FAD altered according to its rotational direction in the settling.

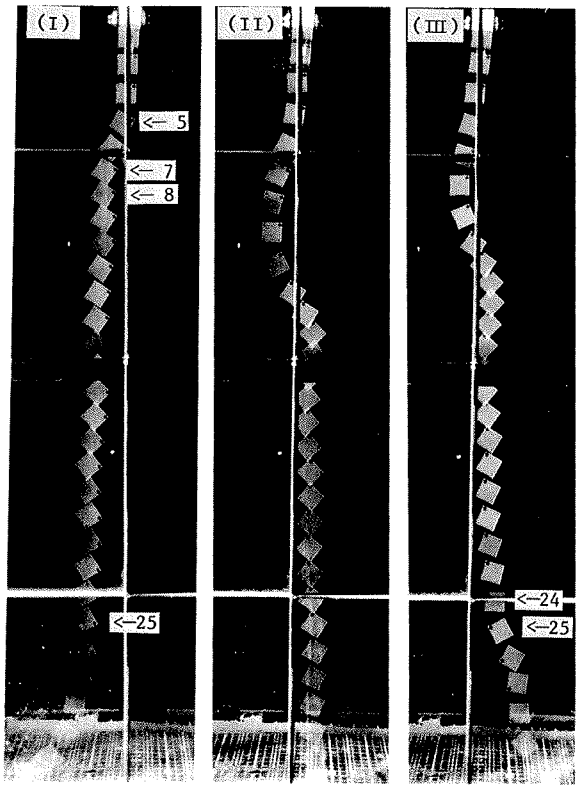

Fig.7 Patterns of settling behavior of FAD model with γ=64%.

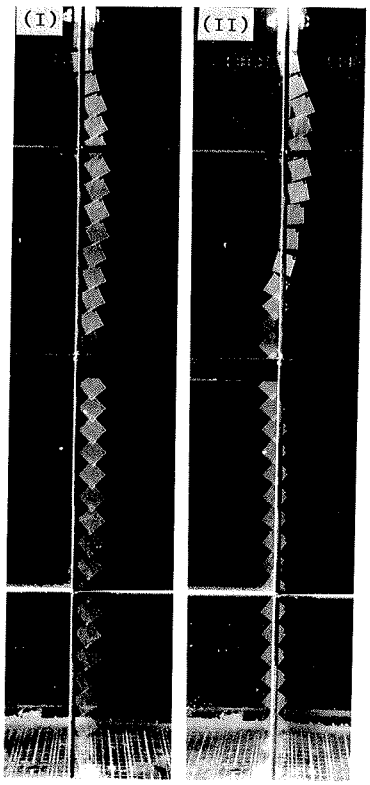

Fig.8 Patterns of settling behavior of FAD model with γ=84%.

Until the 24-th position in Fig.7(III) its motions show the similar patterns observed in Fig.7(II). The FAD settles in the positive and negative direction of horizontal-axis alternatively form the 25-th positions. Fig.8 shows the typical behavior of the settling FAD with γ=84%. From Fig.8, it can be recognized that the fluctuations of the settling FAD in the horizontal direction are smaller in comparison with the γ=64% case. The most stable situation (no oscillatory motion) for the FAD settling can be observed when its surface inclination from the still water surface becomes the angle of about 45°.

Fig.9 shows the calculated behaviors of the settling FAD with γ=64%. In the figure, θ indicates the initial angle from the still water surface at the beginning of the calculation, x/a and y/a are the normalized x, y positions of the FAD center at each calculated position where a is a length of the FAD side. From these calculations, it can be seen that a motion of the settling FAD converges to the stable situation which is recognized in the experiments

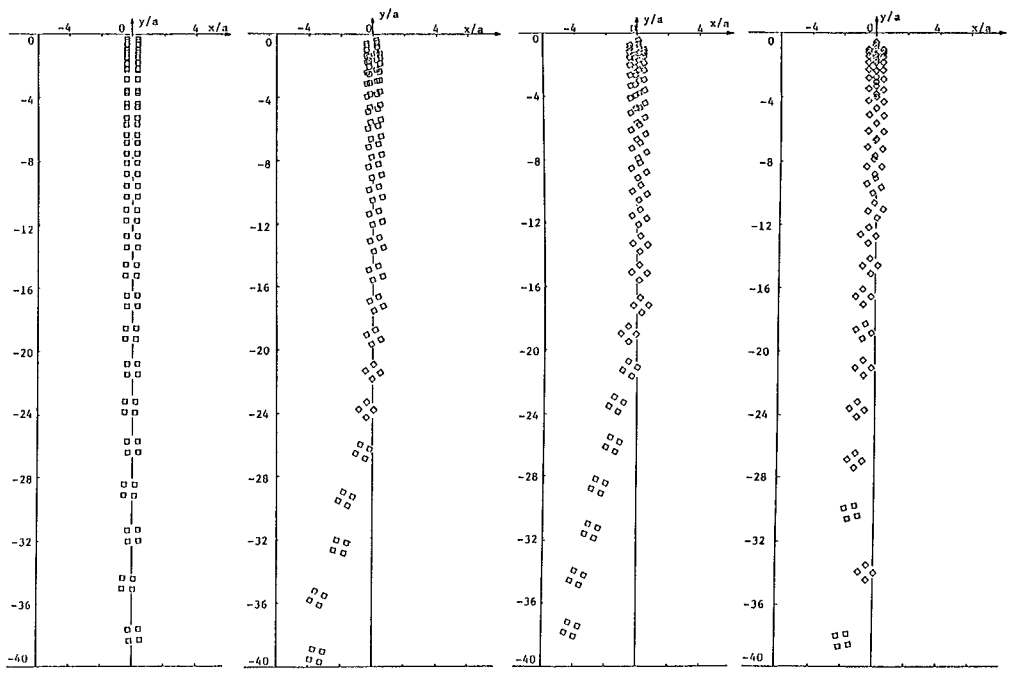

(a) θ=0° (b) θ=15° (c) θ=30° (d) θ=45°

Fig.9 Calculated behaviors of settling FAD model.

(i.e. the angle of the FAD inclination to the still water surface approaches to 45°). In the region y/a<-20 in each calculations, the settling behaviors show the oscillatory motion in the horizontal direction. The present theory can simulate this oscillatory nature of the settling FAD motion which may be induced by the Karman vortex street formed behind the FAD. The significant differences in each calculated results for the different initial angles (θ) were not recognized. This phenomenon has yet been sufficiently clarified in the present study. In addition, the behaviors of the settling FAD in the periodic wave field have to be investigated to verify the present theory. And the impulsive force exerted on the FAD at landing on the bottom may be an another important problem in the future study.

REFERENCE

1) Nakamura,M. : Study on impulsive force on the settling structure at landing, Proc. 22th Conf. on Coastal Engg. in Japan A.S.C.E., 1975, pp.483-487. (in Japanese)

2) Kono,T. : Fundamental study on design of the structure for artificial fishreef, Proc. 24th Conf. on Coastal Engg. in Japan A.S.C.E., 1977, pp.629-633. (in Japanese)
3) Nakamura,T. : Two-dimensional analysis of water wave problems around a body body by source distribution method, Proc. 27th Conf. on Coastal Engg. in Japan A.S.C.E., 1982, pp.462-466. (in Japanese)
4) Roshko,A. : On the drag and shedding frequency of two-dimensional bluff bodies, NACT, TN3169, 1954.
5) Stansby,P.K. : An inviscid model of vortex shedding from a circular cylinder in steady and oscillatory far flows, Proc. Instn Civ. Engrs, Part 2, 1977, pp.865-880.